PUBLICATIONS OF THE ASTRONOMICAL SOCIETY OF THE PACIFIC, **124**:939–955, 2012 September

The Coordinated Radio and Infrared Survey for High-Mass Star Formation (The CORNISH Survey). I. Survey Design

M. G. HOARE,[1] C. R. PURCELL,[1,2,3] E. B. CHURCHWELL,[4] P. DIAMOND,[2,5] W. D. COTTON,[6] C. J. CHANDLER,[7] S. SMETHURST,[2] S. E. KURTZ,[8] L. G. MUNDY,[9] S. M. DOUGHERTY,[10] R. P. FENDER,[11] G. A. FULLER,[2] J. M. JACKSON,[12] S. T. GARRINGTON,[2] T. R. GLEDHILL,[13] P. F. GOLDSMITH,[14] S. L. LUMSDEN,[1] J. MARTÍ,[15] T. J. T. MOORE,[16] T. W. B. MUXLOW,[2] R. D. OUDMAIJER,[1] J. D. PANDIAN,[17] J. M. PAREDES,[18] D. S. SHEPHERD,[7,19] R. E. SPENCER,[2] M. A. THOMPSON,[13] G. UMANA,[20] J. S. URQUHART,[1,5,21] AND A. A. ZIJLSTRA[2]

Received 2012 February 09; accepted 2012 August 15; published 2012 September 19

ABSTRACT. We describe the motivation, design, and implementation of the CORNISH survey, an arcsecond-resolution radio continuum survey of the inner galactic plane at 5 GHz using the Very Large Array (VLA). It is a blind survey coordinated with the northern *Spitzer* GLIMPSE I region covering $10° < l < 65°$ and $|b| < 1°$ at similar resolution. We discuss in detail the strategy that we employed to control the shape of the synthesised beam across this survey, which covers a wide range of fairly low declinations. Two snapshots separated by 4^{h} kept the beam elongation to less that 1.5 over 75% of the survey area and less than 2 over 98% of the survey. The prime scientific motivation is to provide an unbiased survey for ultra-compact H II regions to study this key phase in massive star formation. A sensitivity around 2 mJy will allow the automatic distinction between radio-loud and radio-quiet mid-IR sources found in the *Spitzer* surveys. This survey has many legacy applications beyond star formation, including evolved stars, active stars and binaries, and extragalactic sources. The CORNISH survey for compact ionized sources complements other Galactic plane surveys that target diffuse and nonthermal sources, as well as atomic and molecular phases to build up a complete picture of the interstellar medium in the Galaxy.

Online material: color figures

1. INTRODUCTION

The study of star formation, stellar populations, and Galactic structure is currently being transformed by a new generation of Galactic plane surveys. These surveys have much higher resolution and sensitivity than previous surveys and are conducted at infrared and longer wavelengths that can penetrate the high extinction of the Galactic midplane. They also cover sufficiently wide areas of the plane to provide samples that are large enough to be representative and statistically robust for rare and

[1] School of Physics and Astronomy, University of Leeds, Leeds LS2 9JT, UK; m.g.hoare@leeds.ac.uk.
[2] Jodrell Bank Center for Astrophysics, University of Manchester, Alan Turing Building, Manchester M13 9PL, UK.
[3] Sydney Institute for Astronomy, School of Physics, University of Sydney, NSW 2006, Australia.
[4] Department of Astronomy, University of Wisconsin, 475 North Charter Street Madison, WI 53706.
[5] CSIRO Australia Telescope National Facility, P.O. Box 76, Epping NSW 1710, Australia.
[6] National Radio Astronomy Observatory, 520 Edgemont Road, Charlottesville, VA 22903-2475.
[7] National Radio Astronomy Observatory, P.O. Box O, Socorro, NM 87801-0387.
[8] Centro de Radioastronomía, Universidad Nacinal Autónoma de Méxio-Morelia, Apartado Postal 3-72, C.P. 58090 Morelia, Michoacan, Mexico.
[9] Department of Astronomy, University of Maryland College Park, MD 20742-2421.
[10] National Research Council of Canada, Herzberg Institute for Astrophysics, Dominion Radio Astrophysical Observatory, P.O. Box 248, Penticton, British Columbia V2A 6J9, Canada.
[11] School of Physics and Astronomy, University of Southampton, Southampton SO17 1BJ.
[12] Department of Astronomy , Boston University, 725 Commonwealth Avenue, Boston MA 02215.
[13] Science and Technology Research Institute, University of Hertfordshire, College Lane, Hatfield AL10 9AB, UK.
[14] Jet Propulsion Laboratory, 4800 Oak Grove Drive, Pasadena, CA 91109.
[15] Departamento de Física, Escuela Politécnica Superior de Jaén, Universidad de Jaén, Campus Las Lagunillas, Edificio A3, 23071 Jaén, Spain.
[16] Astrophysics Research Institute, Liverpool John Moores University, Twelve Quays House, Egerton Wharf, Birkenhead CH41 1LD, UK.
[17] Indian Institute of Space Science and Technology, Valiamala, Trivandrum 695547, India.
[18] Departament d'Astronomia i Meteorologia and Institut de Ciències del Cosmos (ICC), Universitat de Barcelona (UB/IEEC), Martí i Franquès 1, Barcelona 08028, Spain.
[19] Square Kilometer Array—Africa, Third Floor, The Park, Park Road, Pinelands 7405, South Africa.
[20] Osservatorio Astrofisico di Catania, via S. Sofia 78, Catania 95123, Italy.
[21] Max Planck Institute for Radio Astronomy, P.O. Box 20 24, Bonn 53010, Germany.

short-lived phases of evolution. Blind surveys that cover contiguous, wide areas also allow the study of phenomena and trends across a large range of scales. A wide wavelength coverage is required to distinguish and characterise the different populations found at both the early and later phases of stellar evolution, and so it is also important to ensure that the same wide areas are covered by all the relevant wavelengths. Here we describe the design and implementation of a new radio continuum survey of the Galactic plane and its role in the context of the other multiwavelength surveys.

1.1. A New Generation of Galactic Plane Surveys

Advances in various widefield technologies have led to a new generation of Galactic plane surveys. Those with relevance here, and to star formation in particular, are listed in Table 1. Leading the way is the GLIMPSE I (Galactic Legacy Infrared Mid-Plane Survey Extraordinaire) survey (Benjamin et al. 2003; Churchwell et al. 2009). This *Spitzer* IRAC Legacy Programme covered the inner Galaxy ($10° < l < 65°$ and $-65° < l < -10°$, $|b| < 1°$) at 3.6, 4.5, 5.8, and 8.0 μm. GLIMPSE is 2 orders of magnitude more sensitive (limit at L-band $(3.6\ \mu\mathrm{m}) \approx 14$–$15$ magnitude, although usually confusion limited) and has 10 times higher spatial resolution (1.4–1.9″) than any previous mid-IR survey. It has catalogued over 49 million sources in a wavelength regime which preferentially selects sources with hot circumstellar dust emission, such as young and evolved stars (e.g., Robitaille et al. 2008). More embedded and cooler sources are the subject of the MIPSGAL survey with *Spitzer* (Carey et al. 2009) and the PACS element of the Hi-GAL survey with *Herschel* (Molinari et al. 2010).

An even deeper probe of the general stellar population is becoming available via the deep near-IR Galactic Plane Survey (GPS) that is part of the UK IR Deep Sky Surveys (UKIDSS) program (Lucas et al. 2008). This survey is about 3 mag more sensitive and has two to three times better resolution than the 2MASS all sky near-IR survey (Skrutskie et al. 2006) and will detect upwards of a billion sources. The addition of near-IR data, where photospheric and scattered light contributions dominate, allows a much better separation and characterization of the general stellar population than from mid-IR colours alone. Near-IR surveys are also being used to map the extinction due to molecular clouds (e.g., Rowles & Froebrich 2009). The optical Hα survey IPHAS (Drew et al. 2005) is providing both stellar characterisation and three-dimensional extinction maps, and tracing nebular emission in less obscured regions of the northern plane with the southern VPHAS+survey[22] scheduled to do the same in the south.

To place the stellar populations in a Galactic context, commensurate studies of the various components of the interstellar medium (ISM) are required. For the study of star formation in particular, the molecular component is provided in part by the BU-FCRAO ^{13}CO 1-0 Galactic Ring Survey (Jackson et al. 2006), which covers over half of the northern GLIMPSE area with extensions over much of the northern midplane (Mottram & Brunt 2010). The mostly optically thin ^{13}CO 1-0 data traces the distribution and dynamics of the cold molecular gas. The cool dust in these molecular clouds can also be mapped via its submillimeter continuum emission. This is currently being achieved with the ATLASGAL survey (Schuller et al. 2009) at 870 μm and BOLOCAM survey at 1100 μm (Aguirre et al. 2011), while the forthcoming JCMT Galactic Plane survey[23] will map the continuum at 450 and 850 μm with higher sensitivity and resolution. Together with the SPIRE element of the Hi-GAL survey with the *Herschel Space Observatory* satellite (Molinari et al. 2010) this will provide temperature and dust emissivity information across the GLIMPSE region.

The more widely distributed atomic hydrogen component is covered by the International GPS at about $1'$ resolution.[24] This is made up of the VLA GPS (VGPS, Stil et al. 2006), Southern GPS (SGPS; McClure-Griffiths et al. 2005) and Canadian GPS (Taylor et al. 2003). A subsection of the plane is covered by the much deeper GALFA survey of H I at $4'$ resolution using the Arecibo telescope (Peek et al. 2011). The H I component traces where most of the mass of interstellar gas is located and its velocity structure. Also, 21 cm absorption lines can help to solve the near/far distance ambiguity in relation to the kinematic distances derived towards the embedded H II regions (Sewilo et al. 2004; Fish et al. 2003) and dense molecular clouds (Jackson et al. 2002; Gibson et al. 2005; Busfield et al. 2006; Roman-Duval et al. 2009). This combination of atomic and molecular kinematic data can therefore provide the three-dimensional Galactic setting of the neutral gas.

The one major component missing from the multiwavelength surveys of the Galaxy is that of the ionized gas. No existing radio continuum survey has sufficient resolution, depth, or coverage to provide the data that would complete the picture of the Galaxy. Ionized gas arises in nebulae and stellar winds around hot stars and is crucial to understanding key phases of the early and late evolution of high- and intermediate-mass stars. Dense, photoionized regions around young and evolved stars are often optically thick with a turnover frequency of around a few GHz, where the radio continuum spectral index α ($S_\nu \propto \nu^\alpha$) changes from the optically thick value of $+2.0$ to the optically thin slope of -0.1. Ionized stellar winds have a positive spectral index $\alpha \sim +0.6$, and so it is also much more efficient to carry out systematic searches for these sources at high frequencies. Furthermore, the resolution should be comparable to the arcsecond resolution of the IR surveys to allow IR counterparts to be uniquely identified. It was to fill this need for a high frequency, high resolution radio continuum survey covering the area of the *Spitzer* survey that the concept of the Co-Ordinated Radio 'N'

[22] See www.vphasplus.org.

[23] See www.jach.hawaii.edu/JCMT/surveys/.

[24] See www.ras.ucalgary.ca/IGPS/.

TABLE 1
GALACTIC PLANE SURVEYS SHOWING THE CONTEXT OF THE CORNISH SURVEY

Survey	Wavelength	Beam (″)	l Coverage (°)	b Coverage (°)	Probe	Reference
IPHAS	Hα	1.7	$30 < l < 210$	$\|b\| < 5$	Nebulae and stars	Drew et al. (2005)
UKIDSS	JHK	0.8	$-2 < l < 230$	$\|b\| < 1$	Stars, Nebulae	Lucas et al. (2008)
VVV	ZYJHK	0.8	$-65 < l < 10$	$\|b\| < 2$	Stars, Nebulae	Minniti et al. (2010)
GLIMPSE	4–8 μm	2	$-65 < l < 65$	$\|b\| < 1$	Stars, Hot Dust	Churchwell et al. (2009)
MSX	8–21 μm	18	All	$\|b\| < 5$	Warm Dust	Price et al. (2001)
MIPSGAL	24,70 μm	6, 20	$-65 < l < 65$	$\|b\| < 1$	Warm Dust	Carey et al. (2009)
AKARI	50–200 μm	30–50	All sky		Cool Dust	White et al. (2009)
Hi-GAL	70–500 μm	10–34	All	$\|b\| < 1$[a]	Cool Dust	Molinari et al. (2010)
JPS	450, 850 μm	8–14	$10 < l < 60$	$\|b\| < 1$	Cool Dust	Moore et al. (2005)
ATLASGAL	850 μm	19	$-60 < l < 60$	$\|b\| < 1.5$	Cool Dust	Schuller et al. (2009)
BOLOCAM	1100 μm	33	$-10 < l < 90$	$\|b\| < 0.5$	Cool Dust	Aguirre et al. (2011)
GRS	^{13}CO 1-0	46	$18 < l < 56$	$\|b\| < 1$	Molecular Gas	Jackson et al. (2006)
MMB	6.7 GHz	192[b]	$-180 < l < 60$	$\|b\| < 2$	Methanol Masers	Green et al. (2009)
HOPS	22 GHz	132[b]	$-180 < l < 60$	$\|b\| < 2$	Water Masers	Walsh et al. (2011)
OH	1.6 GHz	~10	$-45 < l < 45$	$\|b\| < 3$	Hydroxyl Masers	Sevenster et al. (2001)
CORNISH	6 cm	1.5	$10 < l < 65$	$\|b\| < 1$	Compact Ionized Gas	This work
S/V/CGPS	21 cm	60	$-107 < l < 147$	$\|b\| < 1.3$	Atomic Gas	Stil et al. (2006)
MAGPIS	20 cm	5	$5 < l < 48$	$\|b\| < 0.8$	Diffuse Ionized Gas	Helfand et al. (2006)
MGPS-2	35 cm	45	$-115 < l < 0$	$\|b\| < 10$	Diffuse Ionized Gas	Murphy et al. (2007)

[a] Follows warp.
[b] Maser positions are accurate to about 0.1″ after interferometric follow-up.

Infrared Survey for High-mass star formation (CORNISH)[25] survey was conceived.

1.2. Previous Radio Surveys

Many single-dish surveys of the Galactic plane have been carried out at 5 GHz with a resolution of a few arcminutes that is totally inadequate to complement the new generation of IR surveys (e.g., Altenhoff et al. 1978; Haynes et al. 1978; Gregory & Condon 1991; Griffith et al. 1994). Most higher resolution interferometric surveys have been carried out at the relatively low frequency of 1.4 GHz (Zoonematkermani et al. 1990; Becker et al. 1990; Condon et al. 1998; Giveon et al. 2005). Although the multiconfiguration MAGPIS survey (Helfand et al. 2006) and MGPS-2 survey (Murphy et al. 2007) are good for tracing the optically thin thermal emission from extended, evolved H II regions and non-thermal supernova remnants, they are not appropriate for the study of dense, thermal sources due to the unfavourable spectral index and compactness. Becker et al. (1994), with infills by Giveon et al. (2005) and White et al. (2005), have surveyed part of the inner Galaxy ($-10° < l < 42°$, $|b| < 0.4°$) at 5 GHz with the VLA in C configuration, giving a resolution of $4'' \times 9''$. However, these surveys cover only one-fifth of the northern GLIMPSE region, and the spatial resolution is poorer than that of *Spitzer* IRAC, which causes problems with source identification. At this resolution the vast majority of their sources are unresolved, and thus we have no morphological information. In the southern hemisphere, the AT20G survey at 20 GHz and ~30″ resolution (Murphy et al. 2010), primarily designed to study the extragalactic radio source population, is also detecting many H II regions, but again not at sufficient depth or resolution to address the science opened up by current surveys of the Galactic plane at infrared wavelengths.

[25] This acronym derives from the Celtic origins of Hoare and Diamond.

2. SCIENTIFIC MOTIVATION

In this section we describe the various science topics that are addressed by the CORNISH survey. These cover the full range of galactic science from the formation and evolution of stars through to background extragalactic sources.

2.1. High-Mass Star Formation

Our main science driver is the study of the formation of massive stars. These stars impart large amounts of UV radiation, wind energy, strong shocks, and chemically enriched material into the ISM during their lifetime. This is particularly true in starbursts, when they form in dense concentrations (Leitherer 1999). However, relatively little is known about the physics that controls the formation of stars more massive than about 8 $M_\odot$ (10^3 $L_\odot$) and hence about the upper initial mass function (IMF). The fast collapse and contraction time scales and extreme conditions resulting from increased turbulence and radiation pressure makes the theoretical treatment of their formation more challenging than for solar-type stars (e.g., Behrend & Maeder 2001; Yorke & Sonnhalter 2002; McKee & Tan 2003; Bonnell & Bate 2006). Their rarity and predilection to form in dense

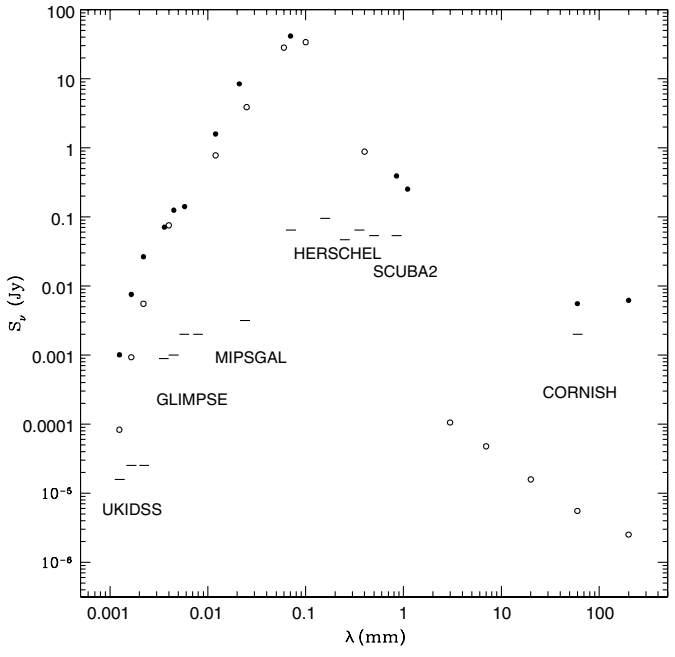

FIG. 1.—Spectral energy distribution (SED) from the near-IR to the radio of an example UCH II region (G042.4343-00.2597, $L = 1.8 \times 10^4\ L_\odot$, $d = 5.0$ kpc, *solid circles*) and MYSO (S140 IRS 1, $L = 0.85 \times 10^4\ L_\odot$, $d = 0.76$ kpc, *open circles*). Sources of the IR data for the H II region can be found in Mottram et al. (2011) and the radio data come from Wood & Churchwell (1989) and Garwood et al. (1988). For S140 IRS 1 the IR data points are discussed in Maud et al. (2012) and the radio points are from Gibb & Hoare (1997) and Schwartz (1989). The flux densities from these objects have been reduced to place them at 15 kpc to reflect early B stars on the far side of the galaxy. The 2 mJy (5σ) sensitivity limit for the CORNISH survey is marked along with the 5σ limits for the UKIDSS, GLIMPSE, MIPSGAL, *Herschel*, and JCMT surveys. Notice that the sensitivities are well matched to the SED of our main targets and that the radio data are vital for distinguishing between the radio-loud UCH IIs and radio-quiet MYSOs.

clusters makes observational studies more challenging and high resolution is a prerequisite (e.g., Beuther et al. 2002).

Current numerical simulations indicate that accretion via a disk can continue despite strong radiation pressure (Krumholz et al. 2009; Kuiper et al. 2010), while submillimeter interferometry reveals evidence of flattened, disklike structures (e.g., Patel et al. 2005; Torrelles et al. 2007) around massive young stellar objects (MYSOs). Although these deeply embedded IR objects are already very luminous, they have yet to ionize the surrounding ISM, most likely due to ongoing accretion keeping them swollen and cool (Hoare & Franco 2007; Hosokawa & Omukai 2009; Davies et al. 2011). MYSOs drive highly collimated ionized jets (Martí et al. 1998; Curiel et al. 2006) and equatorial disk winds (Hoare et al. 1994; Hoare 2006; Gibb & Hoare 2007) which are manifest as compact thermal radio emission (a few mJy for nearby examples) with a spectral index close to $+0.6$. What drives these jets and winds at speeds of a few hundreds of $\mathrm{km\,s^{-1}}$ (e.g., Bunn et al. 1995) is not known. A possible scenario is that the radio jets are accelerated and collimated by an MHD mechanism as in low-mass young stellar objects early on, and these give way to less-collimated radiation pressure dominated flows (Drew et al. 1998) at later stages, akin to the scheme outlined by Beuther & Shepherd (2005).

The strong radio emission from H II regions, formed once the star has contracted down to the main sequence and heated up, is a very useful probe of massive star formation (Hoare et al. 2007). It is unaffected by extinction and can thus be used to measure the formation rate of OB stars right across a galaxy (e.g., Condon, Cotton & Broderick 2002). The radio brightness of H II regions can be used to infer the flux of Lyman continuum photons from the exciting star or cluster and hence constrain the spectral type and mass of the star(s). H II regions provide one of the clearest signatures of spiral structure which can be related to the global distribution of molecular and atomic hydrogen from complementary surveys. This is particularly important in the context of the emerging picture of our Galaxy as having two stellar arms linked to the central bar while having four gaseous star-forming arms (Benjamin 2009).

High-resolution studies of Galactic objects have revealed both large numbers of ultracompact objects (UCH IIs) and a preponderance of cometary morphologies (Wood & Churchwell 1989; Kurtz et al. 1994; Walsh et al. 1998). These studies spawned a reexamination of the dynamical models of H II regions (Van Buren & Mac Low 1992; De Pree, Rodríguez & Goss 1995; Williams, Dyson & Redman 1996). The latest cometary models (Arthur & Hoare 2006) require the young OB star to be located in a density gradient to explain the cometary shape, together with a strong stellar wind to give the limb-brightened appearance and an element of proper motion up the density gradient to reconcile the ionized and molecular velocity structure. Such a picture is consistent with one where the formation of these massive stars was triggered by the passage of an external shock wave through the molecular cloud.

There are many instances where the expansion of H II regions appears to be triggering formation of new episodes of massive star formation (e.g., Deharveng et al. 2005; Urquhart, Morgan & Thompson 2009; Moore et al. 2007; Zavagno et al. 2010; Thompson et al. 2012). This is readily apparent in the 8 μm images from the GLIMPSE survey, where the strong polycyclic aromatic hydrocarbon (PAH) emission delineates the photodissociation region (PDR) at the interface between the ionized region and the molecular cloud. Furthermore, the 24 μm images from MIPSGAL show up the warm dust heated by $L\alpha$ within the ionized zone and correlates well with the radio free-free emission (e.g., Watson et al. 2008). Younger phases such as mid-IR bright MYSOs or maser sources are often seen just ahead of the ionization front, sometimes within IR dark regions (Hoare et al. 2007). What fraction of massive star formation occurs in this way, as opposed to spontaneous collapse, is unclear. Conversely, the action of outflows, expanding H II regions, and stellar winds can also disperse the remaining molecular cloud and quench further star formation (e.g., Franco,

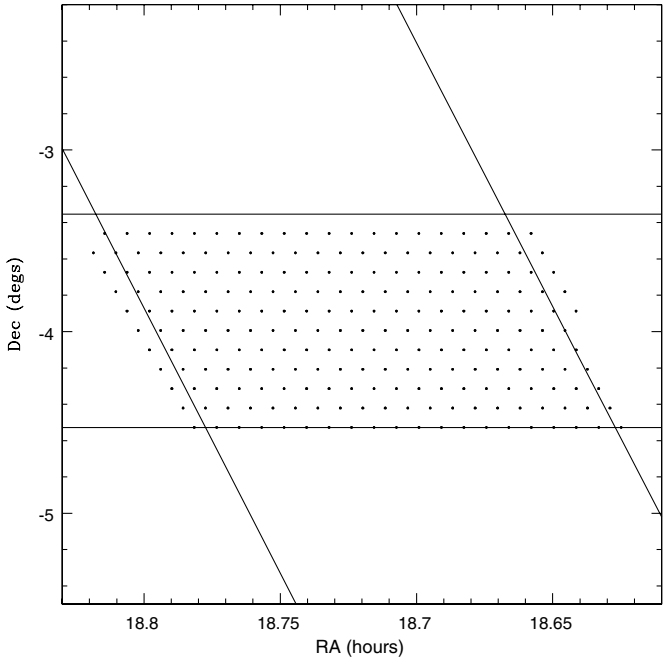

FIG. 2.—Illustration of the pointing pattern for a typical 8 hr observing block. Each dot represents a pointing center. Scans in R. A. started at the bottom of the block and moved upwards before repeating to improve the uv coverage. The diagonal lines represent $b = -1$ and $b = +1$, while the horizontal lines indicate the borders of this block. Notice that pointings extended up to $6.4'$ outside of the nominal survey area to ensure uniform sensitivity within it.

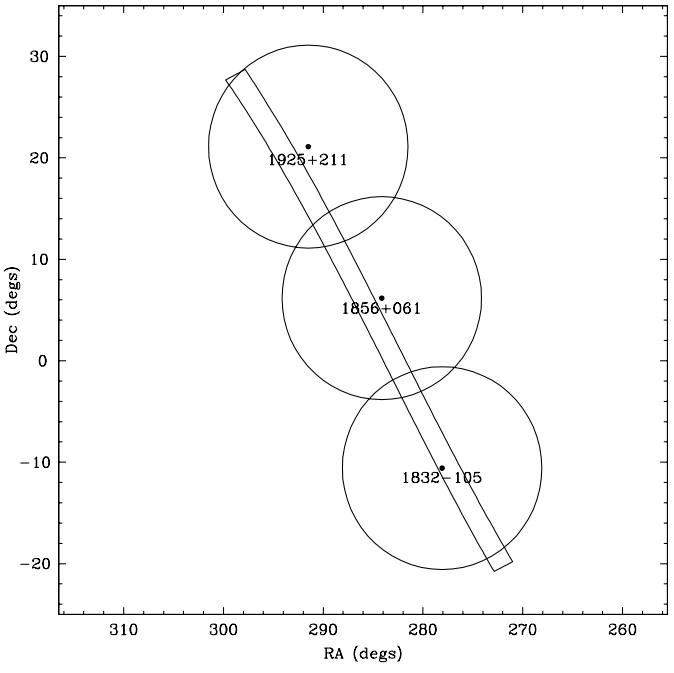

FIG. 3.—The entire survey area with the locations of the three phase calibrators indicated. The circles have radii of 10° showing that these calibrators were sufficient to cover the entire survey area.

Shore, & Tenorio-Tagle 1994). How these opposing feedback mechanisms affect the resultant star formation rate and efficiency is unknown.

Many aspects of massive star formation studies suffer from the lack of a large and unbiased sample of both UCH IIs and MYSOs. Samples based on the IRAS Point Source Catalogue (e.g., Kurtz et al. 1994; Molinari et al.1996; Sridharan et al. 2002) are heavily biased towards bright, isolated sources due to the poor spatial resolution of IRAS, which resulted in confusion in the densest regions of the plane, precisely where massive stars form. The situation for mid-IR bright MYSOs has been alleviated by the Red MSX Source (RMS) survey (Lumsden et al. 2002) that utilized the $18''$ resolution mid-IR survey by the MSX satellite (Price et al. 2001) and high resolution multiwavelength follow-up to yield a large, well-selected sample of MYSOs. This is fairly complete out to about 15 kpc for O star luminosities (Urquhart et al.2011; 2012), and the GLIMPSE survey can easily push this down to the B star range (Robitaille et al. 2008). However, the IR spectral energy distributions (SEDs) of MYSOs and UCH IIs are very similar, and therefore radio continuum data are vital to distinguish these two evolutionary phases (Fig. 1) (e.g., Urquhart et al. 2007). Hence, radio observations are crucial in distinguishing the "radio-quiet" MYSOs from the "radio-loud" UCH II regions. The large numbers of very red objects in the GLIMPSE survey with colors of embedded YSOs makes radio follow-up of each one impractical. The uniform coverage of the CORNISH survey makes this automatic.

The RMS survey also found many UCH II regions, but such IR-selected samples are biased against very embedded objects such as those found in IR dark clouds (IRDCs) (Egan et al. 1998). Many examples of methanol maser sources (Ellingsen 2006), extended green objects (EGOs) (Cyganowski et al. 2008), and faint 24 μm MIPSGAL sources (Rathborne et al. 2010) are showing up in IRDCs. Is there radio continuum emission associated with these very early phases of massive star formation? Cyganowski et al. (2011) performed deep radio continuum observations of a sample of EGOs and found mostly weak or nondetected sources consistent with jets or winds in the diagnostic plots of Hoare & Franco (2007). The rarity of known MYSOs with luminosities above 10^5 $L_\odot$ raises the question of whether early O stars ever go through a detectable mid-IR bright MYSO phase, or whether they manifest themselves firstly as UCH IIs.

TABLE 2

LOG OF OBSERVATIONS

Dates	l ranges observed (°)
2006 Jul 12 to 2006 Sep 16	21.1 to 48.9
2007 Sep 28 to 2007 Oct 6	10.0 to 16.1
2007 Oct 27 to 2008 Apr 2	16.1 to 21.1 and 48.9 to 65.4

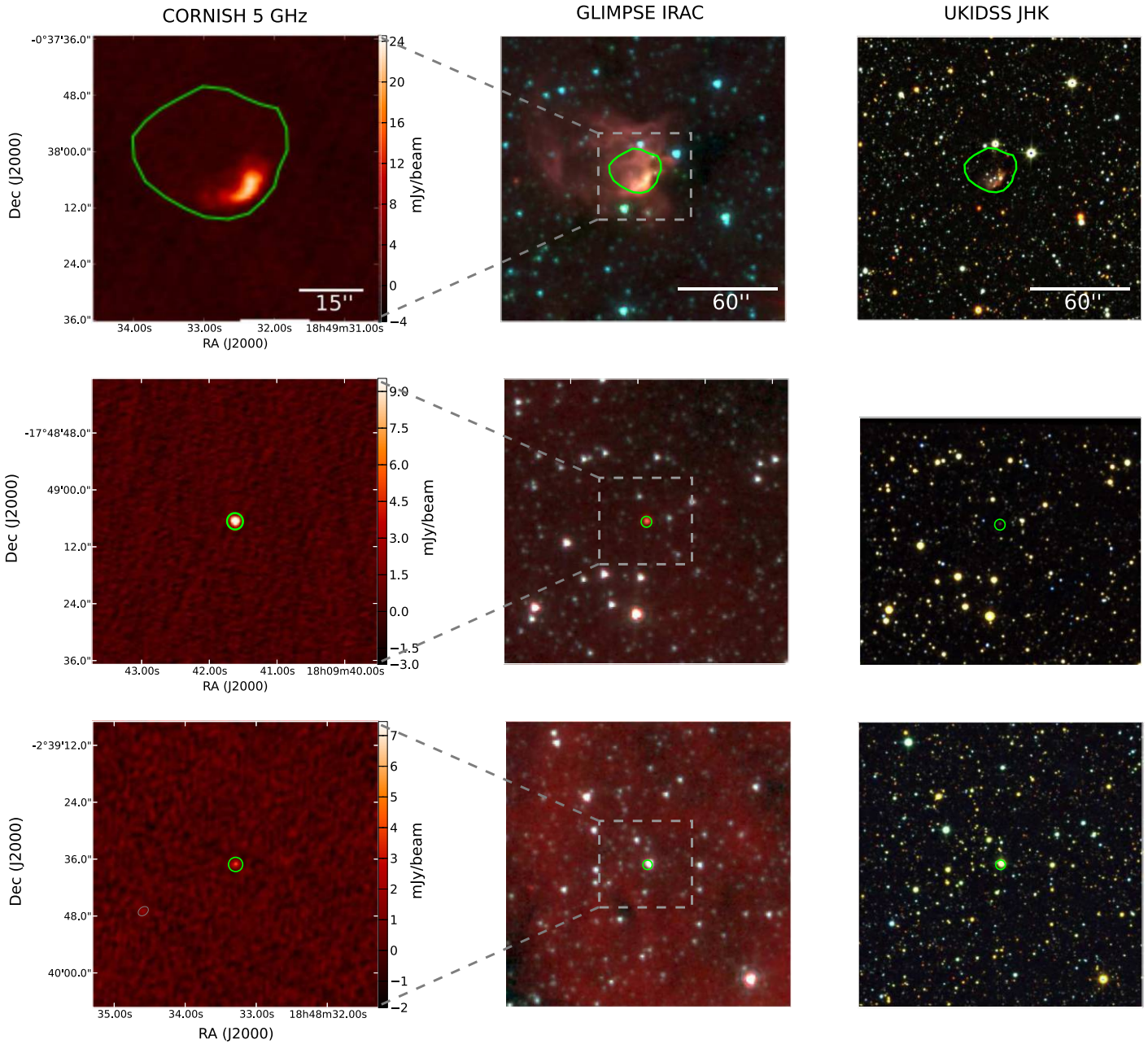

FIG. 4.—Example data from the CORNISH survey alongside three-color images from the *Spitzer* GLIMPSE (3.6, 4.5, and 8.0 μm) and UKIDSS (JHK) surveys. *Top*: A typical cometary H II region, G032.1502 + 00.1329. Notice the good correspondence between the radio emission and the brightest 8 μm emission in the GLIMPSE image. There is also strong extinction ahead of the cometary as expected if the OB star formed in a density gradient. *Middle*: A candidate PN that was previously unknown, G012.3830 + 00.7990. It is clearly seen as an isolated source at 8 μm with a very faint counterpart in the near-IR. In the longer wavelength *Spitzer* MIPSGAL data (not shown here) it is bright at 24 μm but fainter at 70 μm unlike H II regions that are brighter at 70 μm. *Bottom*: A previously unknown radio star, G030.2357 − 00.5719, that has blue colors in the near- and mid-IR. See the electronic edition of the *PASP* for a color version of this figure.

The clean selection function of the CORNISH survey combined with dynamical models and population simulation will allow us to determine the lifetime of this phase as a function of luminosity (e.g., Davies et al. 2011). Together with similar work for MYSOs from the RMS survey and earlier phases from the Hi-GAL and SCUBA2 surveys, this will yield the first comprehensive picture of the evolutionary scheme from high mass star formation. Modelling the flux, size, and shape distributions of the UCH II region population will test the dynamical models of UCH II regions and their relative locations in the dense

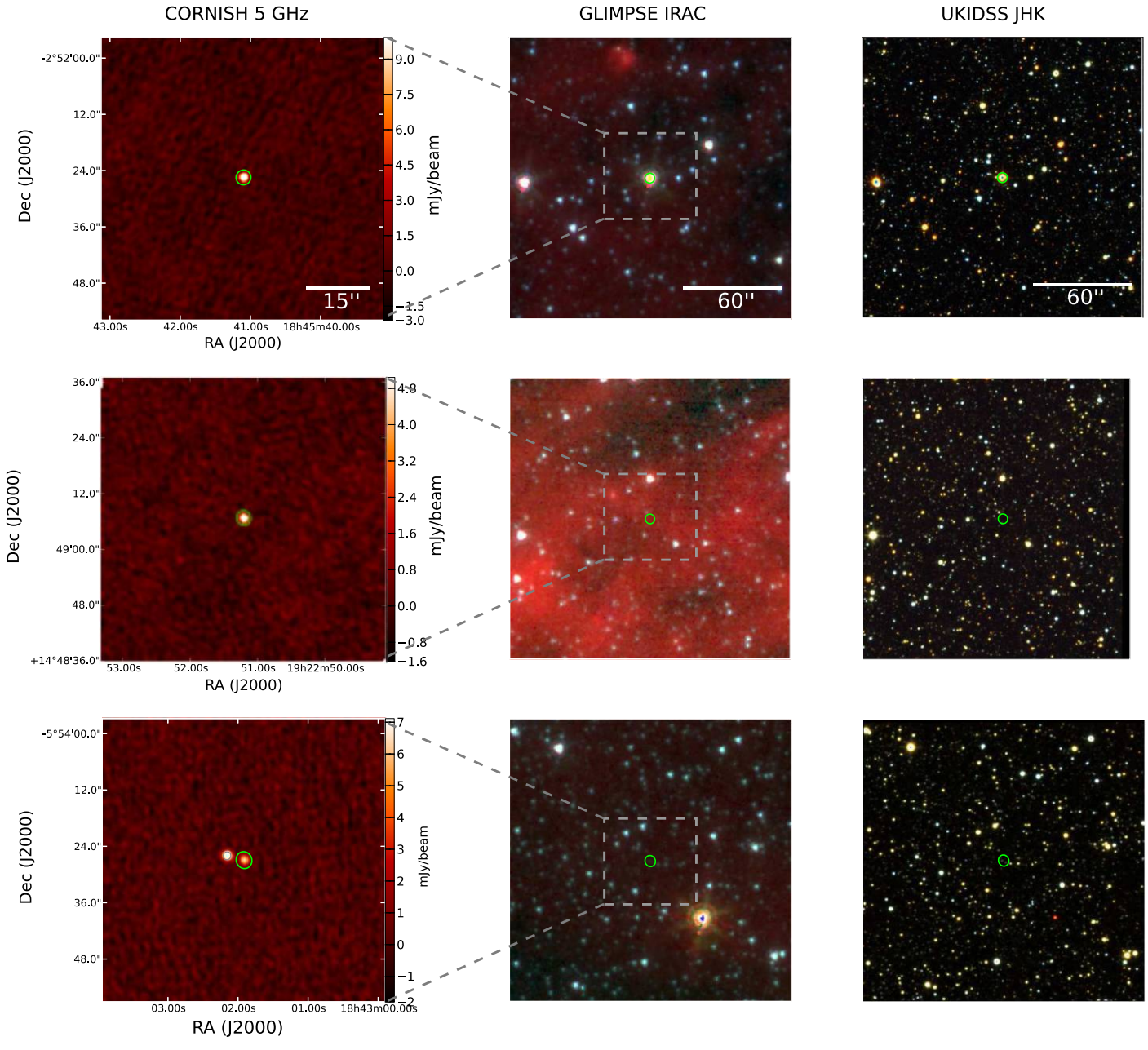

FIG. 5.—Further example data. *Top:* A previously unknown radio star, G029.7188 − 00.0316, that has red colors in the near- and mid-IR. *Middle*: A candidate radio galaxy where we only see one unresolved component, G049.6617 − 00.0543. No counterpart is seen in the IR. *Bottom*: A candidate radio galaxy where we see two unresolved components, G026.7179 − 00.8290. Again, no counterpart is seen in the IR. See the electronic edition of the *PASP* for a color version of this figure.

molecular cloud material will enable statistical tests of triggering scenarios. These tests are only possible from uniform, wide-area surveys with sufficient sensitivity and resolution.

In the high mass star formation context, a spatial resolution of about 1″ is needed in a complementary radio survey for several reasons. Firstly, the IR source density in regions of massive star formation is very high in dense star forming regions. Hence, to accurately identify the IR counterpart to a compact radio source, arcsecond resolution is needed. Secondly, UCH IIs themselves often appear in complexes with separations of a few arcseconds (e.g., Sewilo et al. 2004). Finally, as previous surveys have shown, to reveal the structure of most UCH IIs, a resolution finer than an arcsecond is needed.

2.2. Planetary and Proto-Planetary Nebulae

Zijlstra & Pottasch (1991) estimated that there should be about 23,000 planetary nebulae (PN) in the galaxy, although

only just over 3000 have been identified (Frew & Parker 2010). Combined radio and IRAS searches have been successful in turning up new PN (Van de Steene & Pottasch 1995; Condon, Kaplan, Terzian 1999). A high-resolution radio survey is particularly suited to discovering young, compact PN that are heavily reddened by line-of-sight extinction in the Galactic plane, and we expect about a thousand of these in the survey area. Their radio flux densities are expected to be in the range of 5–50 mJy for typical distances with sizes of a few arcseconds. A complete sample over a large region of the Galactic plane will constrain the density of PN and hence their formation rate and distribution in the Galaxy. This has implications for models of post-AGB (asymptotic giant branch) evolution and mass loss which are not well constrained (e.g., Casassus & Roche 2001).

As in the case of UCH IIs, the immediate progenitors of PN, the proto-PN (PPN), are also radio-quiet since the central star has not yet reached 30,000 K. The radio-quiet PPN will also have very similar mid-IR colors to the radio-loud PN, and so the only way to distinguish them is through their lack of radio emission. This is another illustration of the usefulness of non-detections as well as detections in the radio survey. PPN hold the key to understanding the envelope ejection process and testing the interacting winds models for the shaping of PN (e.g., Mellema & Frank 1995). It is not known whether aspherical mass loss at the end of the AGB is due to AGB star spin-up, detached or common-envelope binaries (Mastrodemos & Morris 1999), or dynamically important magnetic fields (Gardiner & Frank 2001). If we take the birth rate of PN to be about 1 per year (Kwok 2000) and the same for PPN with a PPN lifetime of 1500 years, then we expect about 250 PPN in our survey region.

2.3. Evolved OB Stars

Mass loss from the later evolutionary stages of massive stars (e.g., OB supergiants, Wolf-Rayet stars, and luminous blue variables) is of great importance in the evolution of the ISM in our own and other galaxies, through both the kinetic power deposited by their stellar winds and their strong ionizing radiation fields. Thermal radio emission plays a key role in determining mass loss rates for the evolved massive stars since it arises at large distances from the underlying stars where the outflow has attained a constant velocity (e.g., Wright & Barlow, 1975). Renewed interest in this important input to the ISM has arisen due to clumpiness of the winds (Fullerton et al. 2006). Radio deduced mass loss rates may also provide evidence of the bistability jump and a drop in ratio of wind terminal velocity and the escape velocity (Lamers, Snow & Lindholm 1995), and perhaps also be important to understanding the LBV phase of stellar evolution (Vink & de Koter 2002).

Many of these massive stars exhibit nonthermal emission in addition to the thermal emission from their stellar winds (Bieging et al. 1989), which has been shown to be associated with massive binary systems, with the emission arising where the stellar winds of the two companions collides. The archetype of these colliding-wind binaries is WR140, where the nonthermal emission has led to the determination of all the orbit parameters, the distance, and the wind-momentum and mass ratios (e.g. Dougherty et al. 2005; Dougherty et al. 2011). Among WR stars that exhibit nonthermal emission, over 90% are binaries (Dougherty & Williams, 2000), and there is now evidence that a similar fraction of nonthermal emitters is also observed in O-star binaries (de Becker 2007). Challenges remain for the colliding-wind model. Not all stars with nonthermal emission are found to be binaries, and many binaries exhibit thermal emission, which among short-period systems might be attributed to absorption of the synchrotron power. Alternative mechanisms for accelerating electrons to necessary relativistic speeds have been proposed, e.g., shocks within the stellar winds, that work in single star scenarios.

Studies of both the thermal and nonthermal emitters are limited by the small sample size of the detected systems, and the samples are often biased via spectral type, optical luminosity, or known binary systems. A large, unbiased sample of radio-detected evolved OB stars has previously not been available. Since they inhabit the densest parts of the plane, there are likely many evolved OB stars hidden from optical view by high extinction. For a 5 GHz detection limit of 2 mJy, the limiting radio luminosity is $2.4 \times 10^{18}\ (D/\mathrm{kpc})^2\,\mathrm{erg\,s^{-1}\,Hz^{-1}}$. Using the empirical relationship between $\dot{M}$ and L_{bol} from Garmany & Conti (1984) and the relationship between $L_{6\,\mathrm{cm}}$ and $\dot{M}$ from radio flux from Bieging et al. (1989), we expect this survey to detect all stars with a bolometric luminosity $L_{\mathrm{bol}} \geq 2 \times 10^6\ L_{\odot}$ within $\sim$1 kpc.

2.4. Active Stars

Sensitive radio observations have revealed the ubiquity of high-energy processes across the radio H-R diagram (Güdel 2002). As well as dynamo effects in convective envelopes, high resolution radio observations have revealed large-scale magnetospheric structures in various stellar types, including both low and intermediate mass pre-main-sequence stars. Radio observations reveal dozens of such objects in Orion, and *Chandra* now finds over 1000 active stars in Orion (Garmire et al.2000). With 5 GHz flux densities reaching several tens of mJy, these sources will be detected to several kpc. Particularly intriguing is the role of magnetic fields in intermediate mass pre-main-sequence stars, which are not expected to have convective envelopes and hence large scale dynamos (e.g., Garrington et al.2002). Combined radio, IR, and X-ray studies will reveal how common these magnetic phenomena are.

2.5. Active Binaries

Mass transfer in close binaries often leads to strong activity in radio and other wave bands. RS CVn stars, cataclysmic variables, and others are likely to be detected in the survey. However, the most important class of active binary are the so-called

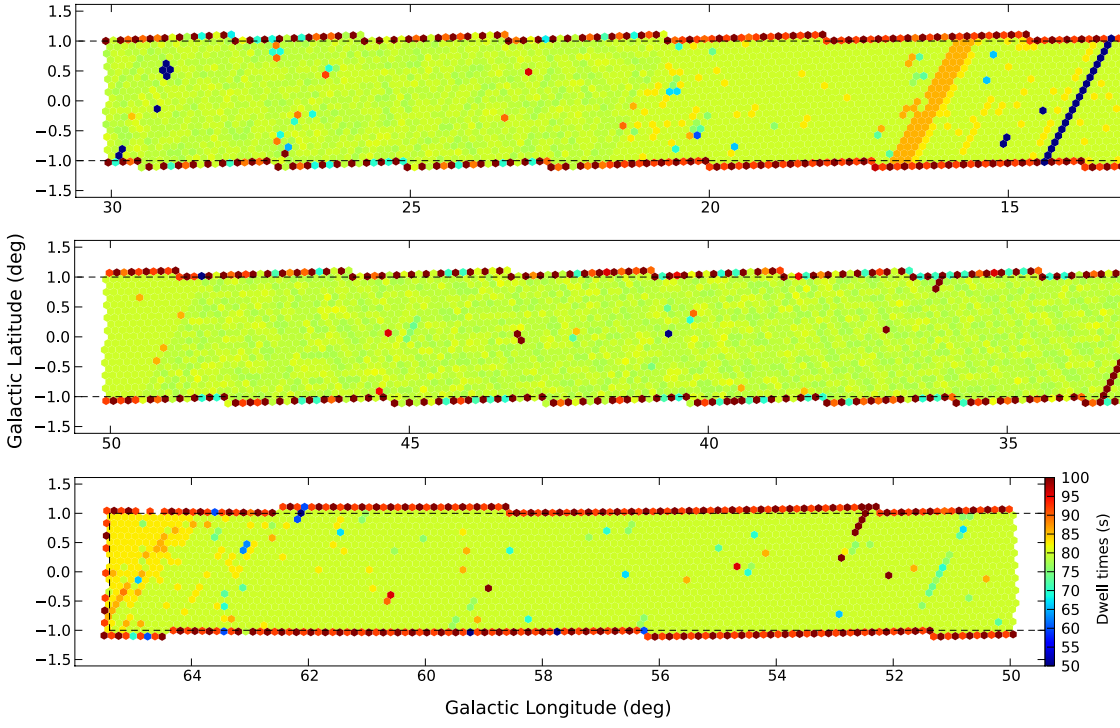

FIG. 6.—Plot showing the dwell time achieved and the final area covered by the CORNISH survey. See the electronic edition of the *PASP* for a color version of this figure.

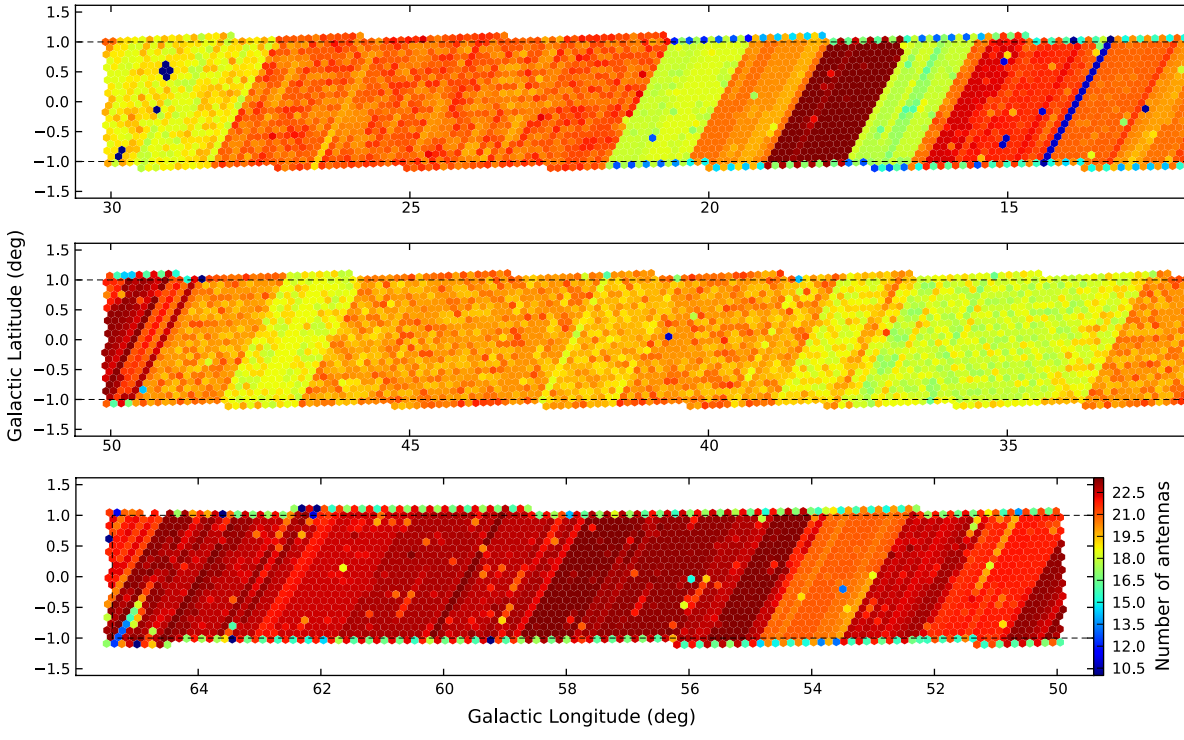

FIG. 7.—Plot showing the effective number of antennas achieved during the CORNISH survey after flagging. See the electronic edition of the *PASP* for a color version of this figure.

microquasars where the accreting object is a black hole or neutron star (Mirabel & Rodríguez 1999; Fender 2002). These produce relativistic jets analogous to AGN where ejections of plasma can be followed in real time (Fender et al. 1999). These objects are perhaps the best laboratories for studying the relativistic jet formation process and test magnetohydrodynamic models (e.g., Meier, Koide, & Uchida 2001). The key signature of these jets is strong synchrotron emission in the radio band, and since they often originate from massive stars one expects to find them close to the Galactic plane and in the locale of giant molecular clouds. In such dense environments, the X-ray and optical signatures of accretion may be heavily absorbed, preventing the detection of accretion by more conventional means. Hence, a coordinated radio and IR survey should uncover many new examples of this phenomena.

There is a strong relationship between the X-ray state and radio behavior in these objects, which has led to the concept of disk-jet coupling. Several black hole candidate objects have flat or inverted radio spectra when in the low/hard X-ray state, indicative of the presence of a self-absorbed compact jet supported by a hot X-ray corona. The jets have been resolved by VLBI in GRS$1915+105$ (Dhawan et al. 2000) and Cygnus X-1 (Stirling et al.2001). When the accretion rate increases, the thermal disk becomes dominant and the X-rays become softer. Radio outbursts often occur during the transition between hard and soft states (Fender, Homan and Belloni 2009) due to the formation of a strong shock in the outflowing jet, and radio interferometer observations are able to follow the evolution of the flow (e.g., Fender et al.1999). Our survey has the resolution to resolve such structures, and at high accretion rates the objects are detectable throughout the disk of the galaxy.

2.6. Extragalactic Sources

There will be a significant number of background extragalactic sources detected during the survey. Using equation A2 in Anglada et al. (1998), which is based on the source count data from Condon (1984), at our completeness level we expect to detect about 2500 extragalactic sources in the 110 square degree area. The vast majority of these radio galaxies will be at too high a redshift to determine distances via H I detections with current telescopes (Magliocchetti et al. 2000; Obreschkow et al. 2009). As well as penetrating the deepest part of the zone of avoidance, these sources will be useful in other respects. The most compact ones are potential phase calibrators for use in future interferometric studies in the Galactic plane. At 5 GHz the CORNISH survey will preferentially pick up flat spectrum sources, which are potential mm-interferometric phase calibrators. Extragalactic sources that are also visible in the optical or near-IR can be used to bring together the radio and optical coordinate reference frames, which is important for multiwavelength high resolution studies in the Galactic plane.

Radio surveys can also deliver a set of extragalactic background sources that can act as pencil beam probes of molecular clouds in follow-up absorption line studies (Greaves & Nyman 1996). Sufficiently strong sources could be used for Zeeman absorption line measurements of the magnetic field strength (Crutcher 1999). For instance, radio sources that lie behind dense, starless molecular cloud cores can be used to probe the initial conditions for star formation in these dense clouds with future sensitive instruments such as the SKA. Polarized background sources can also be used to probe the magnetic field of the Galaxy, individual H II regions, and supernova remnants via Faraday rotation (Taylor et al. 2009). High-frequency data are useful in disentangling components in sources with complex Faraday depth spectra (O'Sullivan et al. 2012).

3. SURVEY SPECIFICATION AND IMPLEMENTATION

The scientific motivation described in the preceding section required a radio continuum survey at around 1 mJy sensitivity, $1''$ resolution, and a frequency significantly higher than the 1.4 GHz traditionally used for surveys. Given the positive spectral index of many of the target sources, then the higher the frequency the better. For VLA receivers, the 8 GHz band would normally be the optimum choice in terms of sensitivity for objects with spectral index around $+0.6$. However, due to the primary beam size, the time required to survey a given area increases as ν^2. Thus a large survey is much more practical at 5 GHz. The VLA 5 GHz sensitivity is similar to that at 8 GHz, but the survey only takes half the time. For a frequency of 5 GHz, the VLA in B configuration delivers a resolution of $1.5''$ that satisfies the scientific requirement. A significant fraction of the area to be surveyed is below declination $-15°$ where it is necessary to switch to the BnA configuration to ensure that the beam elongation does not degrade the resolution. As with any single configuration snapshot survey, the spatial dynamic range is limited and structures larger than about $12''$ in size are not imaged well in the CORNISH survey.

In order to image the full $(8.9')$ primary beam without image degradation due to bandwidth smearing, these observations were carried out in spectral line mode. A 25 MHz bandwidth in 4IF mode was used to maximize the sensitivity. This has eight 3.1 MHz channels, which degrades the peak response by only a few percent at the edge of the primary beam.

To achieve a noise level of 0.3 mJy beam^{-1}, we required a total on-source integration time of 90 s per pointing. This noise level is similar to that used by Wood & Churchwell (1989) and Kurtz et al. (1994) to detect and map UCH II regions throughout the Galaxy. If we use equations (1) and (3) from Kurtz et al. for UCH IIs with an unresolved flux density of 2 mJy placed 20 kpc away, we find that we can detect all objects powered by a B0.5V star or earlier.

To achieve a sensitivity that is uniform across the survey to within 10%, we adopted the NVSS hexagonal pattern of pointing centers (Condon et al.1998). Scaling the NVSS pointing pattern to 5 GHz gives a hexagonal grid separation Δ of $7.4'$. The

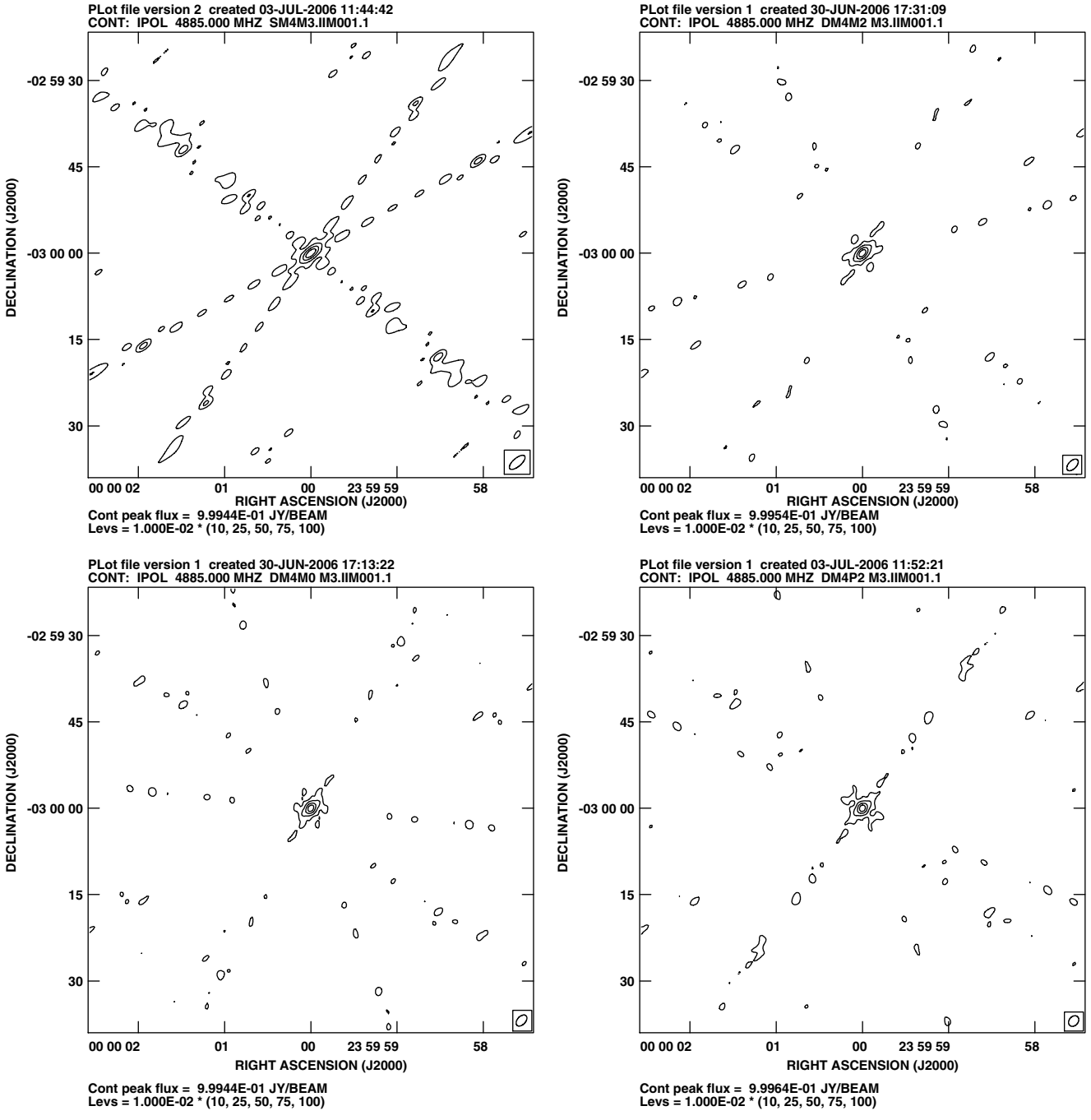

FIG. 8.—*Top left*: Simulated VLA beam for a single 2-minute snapshot at $-4^{\rm h}$ and declination $-3°$. *Top right*: Simulated VLA beam for two 1-minute snapshots at $-4^{\rm h}$ and $-2^{\rm h}$, i.e., separated by $2^{\rm h}$. *Bottom left*: Simulated VLA beam for two 1 minute snapshots at $-4^{\rm h}$ and $0^{\rm h}$, i.e., separated by $4^{\rm h}$. *Bottom right*: Simulated VLA beam for two 1 minute snapshots at $-4^{\rm h}$ and $+2^{\rm h}$, i.e., separated by $6^{\rm h}$.

observations were carried out in the pseudoholography mode developed for the NVSS survey (see Condon et al. 1998), scanning in R.A. between pointings. The separation between pointings in R.A. was $7.4' = (2 \sin 30°)\Delta$, while those in decl. were separated by $6.4' = (\sin 60°)\Delta$. The pointing pattern for a typical observing block is shown in Figure 2. Forty such blocks were completed in 360 hr of time to complete the survey. The survey was spread over two trimesters, with $21° < l < 49°$ being observed in the third quarter of 2006 and the rest in the last quarter of 2007 and the beginning of 2008.

Three phase calibrators ($1832-105$, $1856+061$, and $1925+211$) were used to cover the whole survey with all

TABLE 3
SIMULATED VLA BEAM PARAMETERS FOR THE DIFFERENT SNAPSHOT STRATEGIES SHOWN IN FIG. 8

HA_1 (h.a.)	HA_2 (h.a.)	b_{maj} (″)	b_{min} (″)	b_{maj}/b_{min}
−4	—	3.3	1.4	2.3
−4	−2	2.5	1.4	1.8
−4	0	2.3	1.4	1.6
−4	+2	2.0	1.5	1.3

blocks being within about 10° of one of these (see Fig. 3). This continuity of phase calibrators allowed additional cross-checks of the overall calibration of the survey. A primary flux calibrator $(1331 + 305)$ was observed at the beginning and a secondary flux calibrator $(0137 + 331)$ at the end of each 8 hr observing run. For the BnA observations, 9 rows were completed in shorter 6 hr runs.

Complete coverage of the survey area was achieved and indeed extended to $l = 65.4°$, which was the eventual limit of the GLIMPSE survey. A log of the observation dates can be found in Table 2. Example images, representative of the different types of science discussed in § 2, are presented in Figures 4 and 5, alongside those from the GLIMPSE survey. The complementarity of the similar resolution radio and IR datasets is very apparent.

Figure 6 shows the dwell time across the survey area where the uniform coverage is clearly seen. About 5% of the survey pointings were repeated due to weather or technical problems. Only one scan had a single 45 s pass rather than the usual two (see below) because the repeat scan also failed. Along the edges at $b = -1°$ and 1°, on the end points of scans, the on-source time varied due to the nature of the raster scanning technique. During the survey the VLA antennas were being retrofitted into EVLA antennas, which meant that there were often significantly less than the nominal 27 antennas. In addition to the usual flagging of antennas and baselines due to technical issues this meant that the effective number of antennas varied across the survey as shown in Figure 7.

The median noise level achieved over the survey area was 0.33 mJy beam^{-1} (Purcell et al. 2012) very close to that expected. To determine the nature of the sources in the CORNISH survey it will be very useful to evaluate the spectral index, which requires data at other radio wavelengths. The principal existing source of these data will be the 1.4 GHz plane surveys. For the survey carried out using the VLA in B configuration by White et al. (2005), which overlaps with 91% of the CORNISH survey area, their quoted median noise level is 0.90 mJy beam^{-1}, although there is significant variation over the area. This means that typically a source would need to have a spectral index steeper than −0.8 to be guaranteed to be detected in both. If we take the quoted completeness limit of 13.8 mJy from White et al. (2005), then optically thin H II regions with $\alpha = -0.1$ will need to be stronger than 12 mJy in CORNISH to be also detected in the 1.4 GHz survey. For optically thick H II regions with $\alpha = 2.0$, this rises to 150 mJy. For 55% of the CORNISH area, multiconfiguration VLA 1.4 GHz data exists from the MAGPIS survey (Helfand et al. 2006), with a noise level that is more uniform and 3 times lower than the White et al. (2005) survey. Therefore, for most nonthermal sources in the CORNISH survey with a typical $\alpha = -0.6$, sufficient data exists to characterise their spectral index. However, for thermal sources with a positive spectral index, follow-up observations will be required to measure the spectral index.

4. BEAM SHAPE

To improve the uv coverage and reduce the sidelobes, the 90 s integrations were split into two separate snapshots of 45 s, each separated by 4^h. This strategy was arrived at after simulations were made of the beam shape for various hour angle separations. Figure 8 shows the simulated beams for a single 2 minute snapshot as well as two one-minute snapshots separated by 2^h, 4^h, and 6^h. Table 3 lists the beam parameters for

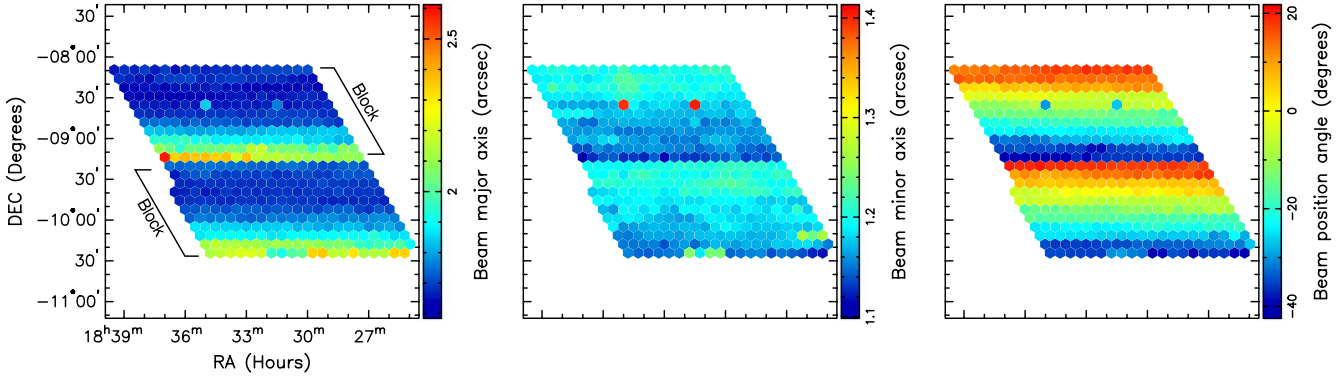

FIG. 9.—The variation in the synthesised beam major axis, minor axis, and position angle over two adjacent observing blocks covering $21.5° < l < 24°$. See the electronic edition of the *PASP* for a color version of this figure.

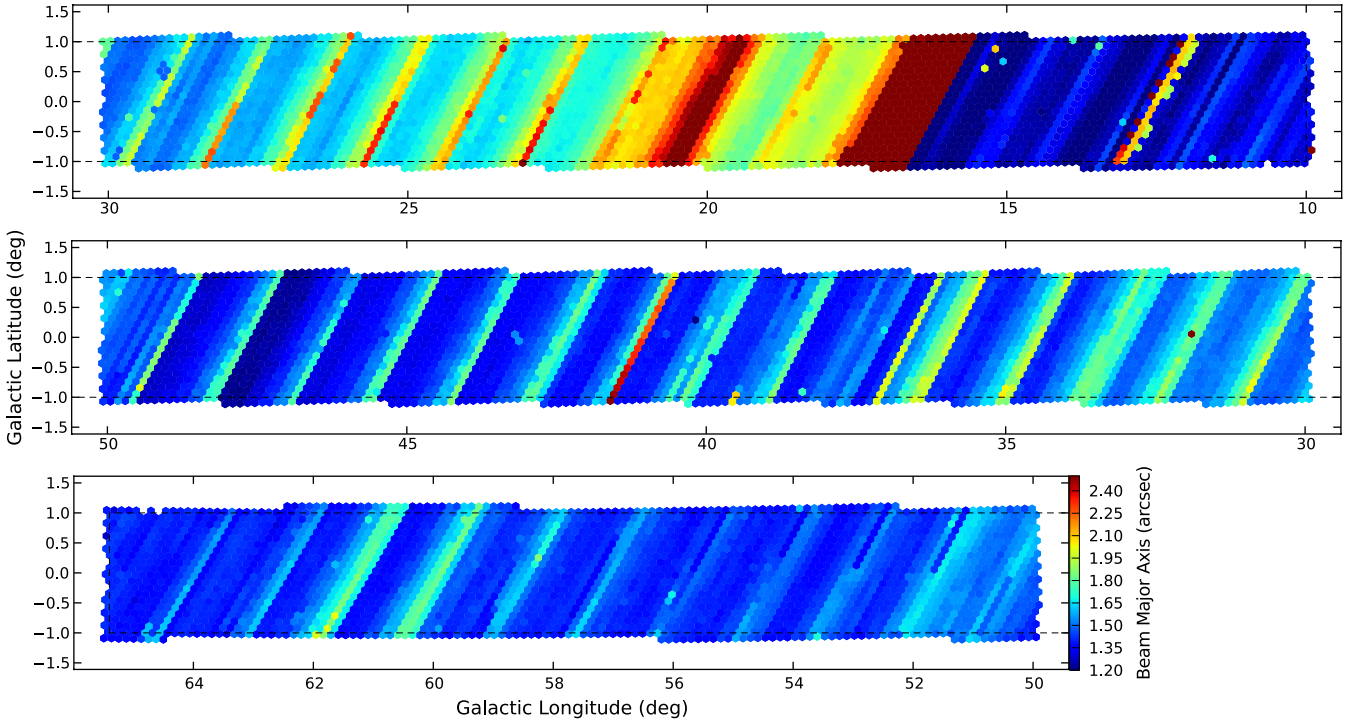

FIG. 10.—Plot showing the major beam axis achieved throughout the survey. See the electronic edition of the *PASP* for a color version of this figure.

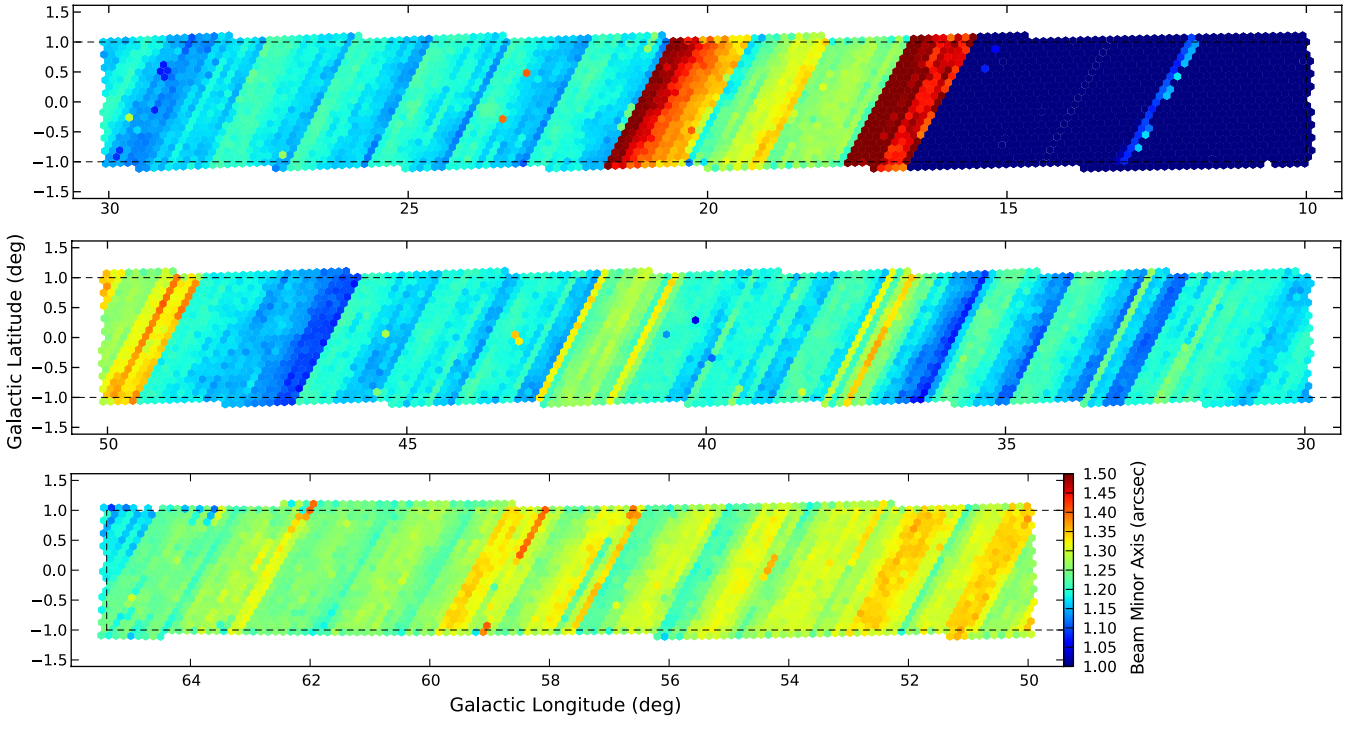

FIG. 11.—Plot showing the minor beam axis achieved throughout the survey. See the electronic edition of the *PASP* for a color version of this figure.

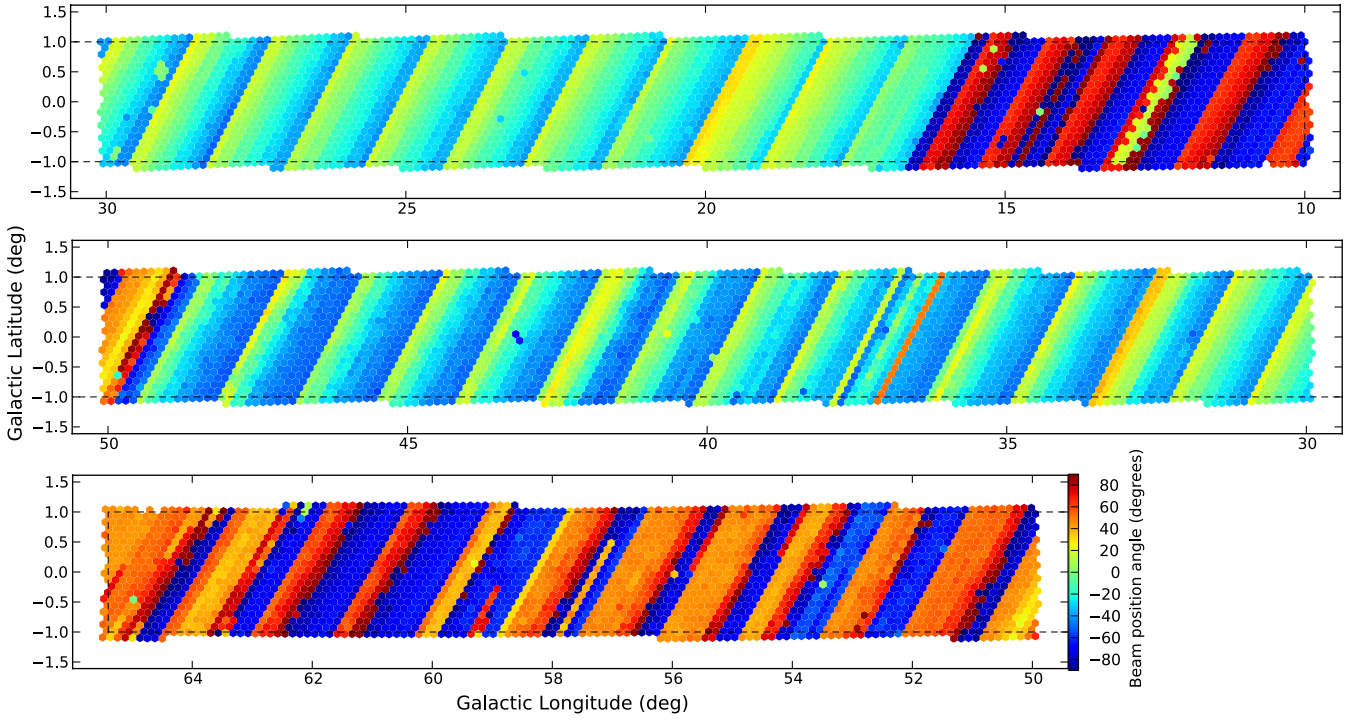

FIG. 12.—Plot showing the beam position angle achieved throughout the survey. See the electronic edition of the *PASP* for a color version of this figure.

each of these simulations. The two snapshots clearly give better beam structure, with the ones separated by 6^{h} giving the best beam shape. However, we used a 4^{h} separation for the survey, as this made implementation and scheduling easier in the 8 hr observing blocks when the Galactic plane was observable.

A typical scanning row contained 20 pointings (see Fig. 2), which including the drive time of about 5 s between pointings took about 17 minutes. Following each scan row a phase calibration of 2 minutes on-source was carried out. Eleven of these rows formed an observing block of about 3.6 hr, after which the whole block was repeated, giving the second snapshot at the appropriate 4^{h} separation. For the BnA observations the observing runs were only 6 hr long due to the lower elevation and the two snapshots were then only 3 hr apart.

The actual beam shape achieved in two consecutive blocks from survey observations carried out during 2006 is shown in Figure 9. This is the synthesised beam (imaged with a robust parameter of zero) after the combination of the two individual 45 s snapshots. The major axis of the beam is slightly worse at the beginning of the blocks (low declination end) than that

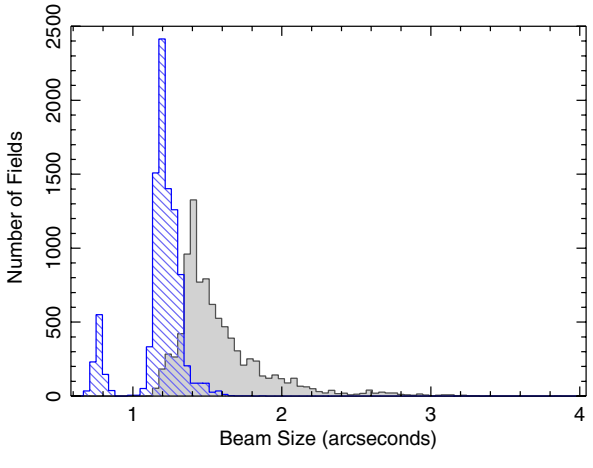

FIG. 13.—Distribution of major (*solid*) and minor (*hatched*) beam axes. See the electronic edition of the *PASP* for a color version of this figure.

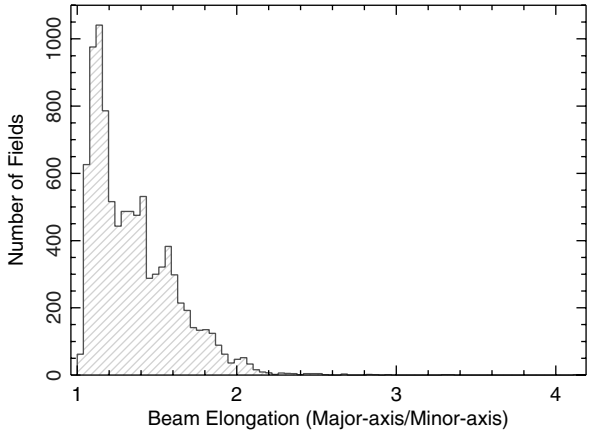

FIG. 14.—Distribution of beam elongation.

predicted in Table 3 for a similar declination. This is because scheduling constraints meant that the 2006 blocks did not quite transit midway through the 8 hr observing session, which resulted in a more asymmetric beam than otherwise achievable. The beam at the end of the block (high declination end) should also have a major axis of about 2.3″ from a combination of the first snapshot at 0^h and a second one at $+4^h$. Another manifestation of the asymmetry in the scheduling is in the beam position angle that rotated from $-40°$ to $+20°$ throughout the block. The minor axis of the beam varied less across the blocks, as expected from Table 3.

The beam parameters over the full survey area are shown in Figures 10–12. Observations conducted during the 2007/2008 were scheduled more symmetrically than in 2006, although the inevitable variation in beam shape is still present. The large change around $l = 16°$ and below is due to the switchover to the BnA configuration for declinations below $-15°$. Here, the position angle of the elongated beam changes from being mostly north-south to an east-west direction.

Histograms of the beam parameters achieved are shown in Figures 13 and 14. The median major axis size achieved was $1.5''$ with a standard deviation of $0.3''$ and a tail up to about $3''$. As expected, the minor axis size has a fairly narrow distribution around $1.2''$ apart from the small number of higher resolution observations due to the BnA configuration data. The distribution of beam elongations shows that 98% of fields have elongations less than 2 and 74% less than 1.5, in agreement with the predictions of Table 3. This shows that in the main the adopted strategy of two snapshots separated by 4^h did deliver the desired constraints on beam shape.

5. CONCLUSIONS

The CORNISH survey is a new, sensitive, high spatial resolution GPS at 5 GHz. It is targeted at compact thermal sources and UCH II regions in particular. Conceived to complement the *Spitzer* GLIMPSE survey, it will systematically address key questions in massive star formation, such as the lifetime and evolution of the UCH II phase as a function of exciting star parameters and environment. Uniform coverage of the northern GLIMPSE region enables the distinction between radio-loud and radio-quiet objects such as MYSOs/UCH IIs and PPN/PN that otherwise have very similar mid-IR colors. Legacy survey science in combination with other recent and upcoming optical, near-IR, far-IR, submillimeter and longer wavelength radio surveys of the plane will be possible with applications in evolved stars, active stars, and active binaries.

Data taking for the CORNISH survey has been completed, and the basic goal of uniformity of coverage achieved. The data reduction, source extraction and statistical properties of the survey and sources will be discussed in the forthcoming paper by Purcell et al. (2012). At that time the catalogue and image data will be publically available online.[26]

We have also achieved the aim of controlling the beam shape across the survey such that the elongation of the synthesised beam is mostly less than 1.5 and nearly always less than 2. This was achieved by using a strategy of two snapshots separated by 4^h. A more uniform and rounder beam could be achieved by more snapshots, but that would increase the overheads and has diminishing returns with the VLA. Our simulations show that snapshots separated by 6^h would have produced a better beam. However, this would have complicated the scheduling of the survey into 8 hr runs and more than likely compromised the very uniform coverage that we ultimately achieved. Such tradeoffs will be the case for any survey with the EVLA at these declinations and for future Galactic plane surveys in particular.

The National Radio Astronomy Observatory is a facility of the National Science Foundation operated under cooperative agreement by Associated Universities, Inc.

[26] See http://www.ast.leeds.ac.uk/cornish.

REFERENCES

Aguirre, J. E., et al. 2011, ApJS, 192, 4
Altenhoff, W. J., Downes, D., Pauls, T., & Schraml, J. 1978, A&AS, 35, 23
Anglada, G., Villuendas, E., Estalella, R., Beltrán, M. T., Rodríguez, L. F., Torrelles, J. M., & Curiel, S. 1998, AJ, 116, 2953
Arthur, S. J., & Hoare, M. G. 2006, ApJS, 165, 283
Becker, R. H., White, R. L., Helfand, D. J., & Zoonematkermani, S. 1994, ApJS, 91, 347
Becker, R. H., White, R. L, McLean, B. J., Helfand, D. J., & Zoonematkermani, S. 1990, ApJ, 358, 485
Behrend, R., & Maeder, A. 2001, A&A, 373, 190
Benjamin, R. A. 2009, in IAU Symp. 254, The Galaxy Disk in Cosmological Context, ed. J. Andersen, J. Bland-Hawthorn, & B. Nordström, (Cambridge: Cambridge University Press), 319
Benjamin, R. A., et al. 2003, PASP, 115, 953
Beuther, H., Schilke, P., Sridharan, T. K., Menten, K. M., Walmsley, C. M., & Wyrowski, F. 2002, A&A, 383, 892
Beuther, H., & Shepherd, D. 2005, in Cores to Clusters: Star Formation with Next Generation Telescopes, ed. M. S. Nanda Kumar, M. Tafalla, & P. Caselli (New York: Springer-Verlag), 105
Bieging, J. H., Abbott, D. C., & Churchwell, E. B. 1989, ApJ, 340, 518
Bonnell, I. A., & Bate, M. R. 2006, MNRAS, 370, 488
Bunn, J. C., Hoare, M. G., & Drew, J. E. 1995, MNRAS, 272, 364
Busfield, A., Purcell, C. R., Hoare, M. G., Lumsden, S. L., Moore, T. J. T., & Oudmaijer, R. D. 2006, MNRAS, 366, 1096
Carey, S. J., et al. 2009, PASP, 121, 76
Casassus, S., & Roche, P. F. 2001, MNRAS, 320, 435
Churchwell, E., et al. 2009, PASP, 121, 213
Condon, J. J. 1984, ApJ, 287, 461

Condon, J. J., Cotton, W. D., Greisen, E. W., Yin, Q. F., Perley, R. A., Taylor, G. B., & Broderick, J. J. 1998, AJ, 115, 1693
Condon, J. J., Cotton, W. D., & Broderick, J. J. 2002, AJ, 124, 675
Condon, J. J., Kaplan, D. L., & Terzian, Y. 1999, ApJS, 123, 219
Crutcher, R. M. 1999, ApJ, 520, 706
Curiel, S., et al. 2006, ApJ, 638, 878
Cyganowski, C., et al. 2008, AJ, 136, 2391
Davies, B., Hoare, M. G., Lumsden, S. L., Hosokawa, T., Oudmaijer, R. D., Urquhart, J. S., Mottram, J. C., & Stead, J. 2011, MNRAS, 416, 972
De Becker, M. 2007, A&A Rev., 14, 171
Deharveng, L., Zavagno, A., & Caplan, J. 2005, A&A, 433, 565
Dhawan, V., Mirabel, I. F., & Rodríguez, L. F. 2000, ApJ, 543, 373
Dougherty, S. M., Beasley, A. J., Claussen, M. J., Zauderer, B. A., & Bolingbroke, N. J. 2005, ApJ, 623, 447
Dougherty, S. M., Trenton, V., & Beasley, A. J. 2011, Bull. Soc. Roy. Sci. Liège, 80, 685
Dougherty, S. M., & Williams, P. M. 2000, MNRAS, 319, 1005
Drew, J. E., Proga, D., & Stone, J. M. 1998, MNRAS, 296, L 6
Drew, J. E., et al. 2005, MNRAS, 362, 753
De Pree, C. G., Rodríguez, L. F., & Goss, W. M. 1995, Rev. Mex. AA, 31, 39
Egan, M. P., Shipman, R. F., Price, S. D., Carey, S. J., Clark, F. O., & Cohen, M. 1998, ApJL, 494, L 199
Ellingsen, S. P. 2006, ApJ, 638, 241
Fender, R. 2002, LNP, 589, 101
Fender, R. P., Garrington, S. T., McKay, D. J., Muxlow, T. W. B., Pooley, G. G., Spencer, R. E., Stirling, A. M., & Waltman, E. B. 1999, MNRAS, 304, 865
Fender, R. P., Homan, J., & Belloni, T. W. 2009, MNRAS, 396, 1370
Fish, V. L., Reid, M. J., Wilner, D. J., & Churchwell, E. 2003, ApJ, 587, 701
Franco, J., Shore, S. N., & Tenorio-Tagle, G. 1994, ApJ, 436, 795
Frew, D. J., & Parker, Q. A. 2010, PASA, 27, 129
Fullerton, A. W., Massa, D. L., & Prinja, R. K. 2006, ApJ, 637, 1025
Garmany, C. D., & Conti, P. S. 1984, ApJ, 284, 705
Garmire, G., Feigelson, E. D., Broos, P., Hillenbrand, L. A., Pravdo, S. H., Townsley, L., & Tsuboi, Y. 2000, AJ, 120, 1426
Gardiner, T. A., & Frank, A. 2001, ApJ, 557, 250
Garrington, S. T., van Langevelde, H. J., Campbell, R. M., & Gunn, A. 2002, in Proc. sixth European VLBI Network Symp., ed. E. Ros, R. W. Porcas, A. P. Lobanov, & J. A. Zensus (Bonn: Max-Planck-Institut für Radioastronomie), 259
Garwood, R. W., Perley, R. A., Dickey, J. M., & Murray, M. A. 1988, AJ, 96, 1655
Gibb, A. A., & Hoare, M. G. 2007, MNRAS, 380, 246
Gibson, S. J., Taylor, A. R., Higgs, L. A., Brunt, C. M., & Dewdney, P. E. 2005, ApJ, 626, 195
Giveon, U., Becker, R. H., Helfand, D. J., & White, R. L. 2005, AJ, 129, 348
Greaves, J. S., & Nyman, L.-Å. 1996, A&A, 305, 950
Green, J., et al. 2009, MNRAS, 392, 783
Gregory, P. C., & Condon, J. J. 1991, ApJS, 75, 1011
Griffith, M. R., Wright, A. E., Burke, B. F., & Ekers, R. D. 1994, ApJS, 90, 179
Güdel, M. 2002, ARA&A, 40, 217
Haynes, R. F., Caswell, J. L., & Simons, L. W. J. 1978, Australian J. Phys. Astrophys. Suppl., 45, 1
Helfand, D. J., Becker, R. H., White, R. L., Fallon, A., & Tuttle, S. 2006, AJ, 131, 2525
Hoare, M. G. 2006, ApJ, 649, 846
Hoare, M. G., Drew, J. E., Muxlow, T. B., & Davis, R. J. 1994, ApJ, 421, L 51
Hoare, M. G., & Franco, J. 2007, in Diffuse Matter from Star Forming Regions to Active Galaxies, ed. T. W. Hartquist, J. M. Pittard, & S. A. E. G. Falle. (Dordrecht: Springer), 61, (astro-ph/0711.4912)
Hoare, M. G., Kurtz, S. E., Lizano, S., Keto, E., & Hofner, P. 2007, in Protostars and Planets V, ed. B. Reipurth, D. Jewitt, & K. Keil, (Tuscon: University of Arizona Press), 181
Hosokawa, T., & Omukai, K. 2009, ApJ, 691, 823
Jackson, J. M., Bania, T. M., Simon, R., Kolpak, M., Clemens, D. P., & Heyer, M. 2002, ApJ, 566, L 81
Jackson, J. M., et al. 2006, ApJS, 163, 145
Krumholz, M. R., Klein, R. I., McKee, C. F., Offner, S. S. R., & Cunningham, A. J. 2009, Science, 323, 754
Kuiper, R., Klahr, H., Beuther, H., & Henning, T. 2010, ApJ, 722, 1556
Kurtz, S., Churchwell, E., & Wood, D. O. S. 1994, ApJS, 91, 659
Kwok, S. 2000, The Origin and Evolution of Planetary Nebulae (Cambridge: Cambridge University Press)
Lamers, H. J. G. L. M., Snow, T. P., & Lindholm, D. M. 1995, ApJ, 455, 269
Leitherer, C. 1999, in IAU Symp. 186, Galaxy Interactions at Low and High Redshift, ed. J. E. Barnes, & D. B. Sanders, (Cambridge: Cambridge University Press), 243
Lucas, P. W., et al. 2008, MNRAS, 391, 136
Lumsden, S. L., Hoare, M. G., Oudmaijer, R. D., & Richards, D. 2002, MNRAS, 336, 621
Magliocchetti, M., Maddox, S. J., Wall, J. V., Benn, C. R., & Cotter, G. 2000, MNRAS, 318, 1047
Martí, J., Rodríguez, L. F., & Reipurth, B. 1998, ApJ, 502, 337
Mastrodemos, N., & Morris, M. 1999, ApJ, 523, 357
Maud, L. T., Hoare, M. G., Gibb, A. G., Shepherd, D., & Indebetouw, R. 2012, MNRAS, submitted
McClure-Griffiths, N., Dickey, J. M., Gaensler, B. M., Green, A. J., Haverkorn, M., & Strasser, S. 2005, ApJS, 158, 178
McKee, C., & Tan, J. 2003, ApJ, 585, 850
Meier, D. L., Koide, S., & Uchida, Y. 2001, Science, 291, 84
Mellema, G., & Frank, A. 1995, MNRAS, 273, 401
Minniti, D., et al. 2010, NewA, 15, 433
Mirabel, I. F., & Rodríguez, L. F. 1999, ARA&A, 37, 409
Molinari, S., Brand, J., Cesaroni, R., & Palla, F. 1996, A&A, 308, 573
Molinari, S., et al. 2010, PASP, 122, 314
Moore, T. J. T., Bretherton, D. E., Fujiyoshi, T., Ridge, N. A., Allsopp, J., Hoare, M. G., Lumsden, S. L., & Richer, J. S. 2007, MNRAS, 379, 663
Moore, T. J. T., et al. 2005, in Protostars and Planets V, ed. B. Reipurth, D. Jewitt, & K. Keil (Tuscon: University of Arizona Press), 8370
Mottram, J. C., & Brunt, C. M. 2010, in The Dynamic Interstellar Medium: A Celebration of the Canadian Galactic Plane Survey, ed. R. Kothes, T. L., Landecker, & A. G. Willis (San Francisco: Astronomical Society of the Pacific), 98
Mottram, J. C., et al. 2011, A&A, 525, 149
Murphy, T., Mauch, T., Green, A., Hunstead, R. W., Piestrzynska, B., Kels, A. P., & Sztajer, P. 2007, MNRAS, 382, 382
Murphy, T., et al. 2010, MNRAS, 402, 2403
O'Sullivan, S. P., et al. 2012, MNRAS, 421, 3300

Obreschkow, D., Klöckner, H.-R., Heywood, I., Levrier, F., & Rawlings, S. 2009, ApJ, 703, 1890
Patel, N. A., et al. 2005, Nature, 437, 109
Peek, J. E. G., et al. 2011, ApJS, 194, 20
Price, S. D., Egan, M. P., Carey, S. J., Mizuno, D. R., & Kuchar, T. A. 2001, AJ, 121, 2819
Purcell, C. R., et al. 2012, ApJS, submitted
Rathborne, J. M., Jackson, J. M., Chambers, E. T., Stojimirovic, I., Simon, R., Shipman, R., & Frieswijk, W. 2010, ApJ, 715, 310
Robitaille, T. P., et al. 2008, AJ, 136, 2413
Roman-Duval, J., Jackson, J. M., Heyer, M., Johnson, A., Rathborne, J., Shah, R., & Simon, R. 2009, ApJ, 699, 1153
Rowles, J., & Froebrich, D. 2009, MNRAS, 395, 1640
Schuller, F., et al. 2009, A&A, 504, 415
Schwartz, P. R. 1989, ApJ, 338, L 25
Sevenster, M. N., van Langevelde, H. J., Moody, R. A., Chapman, J. M., Habing, H. J., & Killeen, N. E. B. 2001, A&A, 366, 481
Sewilo, M., Churchwell, E., Kurtz, S., Goss, W. M., & Hofner, P. 2004, ApJ, 605, 285
Skrutskie, M. F., et al. 2006, AJ, 131, 1163
Sridharan, T. K., Beuther, H., Schilke, P., Menten, K. M., & Wyrowski, F. 2002, ApJ, 566, 931
Stil, J. M., et al. 2006, AJ, 132, 1158
Stirling, A. M., Spencer, R. E., de la Force, C. J., Garrett, M. A., Fender, R. P., & Ogley, R. N. 2001, MNRAS, 327, 1273
Taylor, A. R., et al. 2003, AJ, 125, 3145
Taylor, A. R., Stil, J. M., & Sunstrum, C. 2009, ApJ, 702, 1230
Thompson, M. A., Urquhart, J. S., Moore, T. J. T., & Morgan, L. K. 2012, MNRAS, 421, 408
Torrelles, J. M., Patel, N. A., Curiel, S., Ho, P. T. P., Garay, G., & Rodríguez, L. F. 2007, ApJ, 666, L 37
Urquhart, J. S., Busfield, A. L., Hoare, M. G., Lumsden, S. L., Clarke, A. J., Moore, T. J. T., Mottram, J. C., & Oudmaijer, R. D. 2007, A&A, 461, 11
Urquhart, J. S., Morgan, L. K., & Thompson, M. A. 2009, A&A, 497, 789
Urquhart, J. S., et al. 2011, MNRAS, 410, 1237
Urquhart, J. S., et al. 2012, MNRAS, 420, 1656
Van Buren, D., & Mac Low, M.-M. 1992, ApJ, 394, 534
Van de Steene, G. C., & Pottasch, S. R. 1995, A&A, 299, 238
Vink, J. S., & de Koter, A. 2002, A&A, 393, 543
Walsh, A. J., Burton, M. G., Hyland, A. R., & Robinson, G. 1998, MNRAS, 301, 640
Walsh, A. J., et al. 2011, MNRAS, 416, 1764
Watson, C., et al. 2008, ApJ, 681, 1341
White, G. J., et al. 2009, ASPC, 418, 67
White, R. L., Becker, R. H., & Helfand, D. J. 2005, AJ, 130, 586
Williams, J. R., Dyson, J. E., & Redman, M. P. 1996, MNRAS, 280, 661
Wood, D. O. S., & Churchwell, E. 1989, ApJS, 69, 831
Wright, A. E., & Barlow, M. J. 1975, MNRAS, 170, 41
Yorke, H. W., & Sonnhalter, C. 2002, ApJ, 569, 846
Zavagno, A., et al. 2010, A&A, 518, L 101
Zijlstra, A. A., & Pottasch, S. R. 1991, A&A, 243, 478
Zoonematkermani, S., Helfand, D. J., Becker, R. H., White, R. L., & Perley, R. A. 1990, ApJS, 74, 181